

A Gradient-Based Capacity Accreditation Framework in Resource Adequacy: Formulation, Computation, and Practical Implications

Qian Zhang, Feng Zhao, Gord Stephen, Chanan Singh, Le Xie

Abstract—Probabilistic resource adequacy assessment is a cornerstone of modern capacity accreditation. This paper develops a gradient-based framework, in which capacity accreditation is interpreted as the directional derivative of a probabilistic resource adequacy metric with respect to resource capacity, that unifies two widely used accreditation approaches: Effective Load Carrying Capability (ELCC) and Marginal Reliability Impact (MRI). Under mild regularity conditions, we show that marginal ELCC and MRI yield equivalent accreditation factors, while their numerical implementations exhibit markedly different computational characteristics. Building on this framework, we demonstrate how infinitesimal perturbation analysis enables up to a $1000 \times$ speedup in gradient estimation for capacity accreditation, and we implement gradient-informed search algorithms that significantly accelerate ELCC computations relative to standard bisection methods. Large-scale Monte Carlo experiments show that MRI achieves substantial runtime reductions compared to ELCC and exhibits greater robustness to perturbation step-size selection. These results provide practical guidance for implementing efficient and scalable capacity accreditation in large-scale power systems.

Index Terms—Resource adequacy, effective load carrying capability, marginal reliability impact, capacity accreditation

I. INTRODUCTION

To ensure power system reliability and cost-efficiency under a rapidly changing resource mix, many regions have been reforming *capacity accreditation* frameworks to improve fairness and accuracy, both in market-based settings [1], [2], [3] and in centralized planning frameworks [4], [5]. A key motivation is that legacy heuristic approaches, such as outage-rate-discounted unforced capacity (UCAP) for thermal units and historical average output for intermittent resources, can mischaracterize reliability contributions as systems become increasingly weather-driven and exhibit stronger cross-resource correlations. In principle, accredited capacities from different resource types are treated as indistinguishable for meeting system capacity requirements, implying that one megawatt of capacity credit should provide the same contribution to system resource adequacy (RA) independent of the underlying technology.

To address these challenges, two *gradient-based* probabilistic capacity accreditation methods are now widely used (or

Qian Zhang and Le Xie are with the School of Engineering and Applied Sciences, Harvard University, Allston, USA. Feng Zhao is with the ISO New England Inc., Holyoke, MA, USA. Gord Stephen is with the Department of Electrical and Electronic Engineering, Imperial College London, SW7 2BU London, UK. Chanan Singh is with the Department of Electrical and Computer Engineering, Texas A&M University, College Station, USA. (correspondence e-mail: qianzhang@g.harvard.edu).

under active consideration): *Effective Load Carrying Capability* (ELCC) and *Marginal Reliability Impact* (MRI). Both quantify a resource's contribution to RA by evaluating changes in a chosen reliability metric under a probabilistic loss-of-load simulation model. Moreover, when the reliability metric is selected as Expected Unserved Energy (EUE), marginal ELCC yields the same accreditation value as MRI under standard regularity conditions [6]. Despite this conceptual relationship, the literature has not yet established a rigorous mathematical formulation, nor provided a clear comparison of the computational complexity between ELCC and MRI in large-scale system applications.

A resource's ELCC is defined as the greatest constant firm load that can be added to the system *after* adding the resource while maintaining the same reliability level [7]. Capacity accreditation based on ELCC is obtained by normalizing the load-carrying capability by the nameplate quantity of the resource addition, whether evaluated for an entire resource class (average ELCC) or for an incremental unit (marginal ELCC)¹. In contrast, MRI is defined as the marginal impact of a small capacity variation on system EUE [8]. Unlike ELCC (measured in MW), MRI has units of hours per study period, and the MRI-based accreditation is defined as the normalized MRI by the MRI of a *perfect* reference resource [6].

ELCC and MRI are evaluated through probabilistic assessment of stochastic power systems with heterogeneous resources and discrete outage and availability events, implemented in practice using probabilistic resource adequacy assessment (RAA) simulators such as GE-MARS [9] and PRAS [10]. A substantial body of RA research has focused on the definition and evaluation of reliability metrics [11], [12], Monte Carlo sample size selection [13], and the integration of emerging resources such as variable generation and storage [14], [15]. These efforts primarily target accurate estimation of system-level reliability outcomes under uncertainty.

Capacity accreditation adds an additional layer of difficulty: rather than only evaluating reliability, it requires quantifying how reliability changes under marginal resource additions. This is a *gradient estimation* problem in a stochastic simulation environment, and the broader simulation literature has developed multiple estimator families, such as finite-difference methods, infinitesimal perturbation analysis, and likelihood-ratio approaches, each with distinct bias-variance and implementability tradeoffs [16], [17]. However, rigorous

¹Unless otherwise stated, “ELCC” in this paper refers to *marginal* ELCC.

formulations that connect these gradient estimation concepts to capacity accreditation, together with large-scale computational validation under realistic RA simulation settings, remain limited in the power systems literature [18].

The contributions of this paper are fourfold. First, we formulate ELCC- and MRI-based capacity accreditation within a unified gradient-based framework by casting accreditation as directional derivatives on a well-defined probability space, and we state explicit assumptions under which marginal ELCC and MRI yield equivalent accreditation factors (Sections II and III). Second, we introduce an infinitesimal perturbation analysis (IPA) perspective to characterize and interpret the meaning of gradients in capacity accreditation, to clarify when unbiased pathwise gradient estimators are available. IPA can be used to reduce computational cost by enabling gradient-based capacity accreditation to be obtained from a single simulation run (Section IV). Third, focusing on perturbation-based implementations that dominate current practice, we identify key computational challenges in simulation-based accreditation and provide a comparative complexity analysis showing why ELCC requires iterative root-finding while MRI can be computed in a single pass (Section V). Finally, using large-scale numerical studies, we quantify computation time and numerical sensitivity for ELCC and MRI across perturbation step sizes and baseline reliability levels, thereby illustrating practical implications for implementing scalable accreditation in modern systems (Section VI).

II. PRELIMINARIES AND DEFINITIONS

A. System Descriptions

Let \mathcal{T} denote the set of all hours in a year (or the study periods of interest), \mathcal{D} the set of all days, and Ω the set of all possible year-long scenarios for the system under study, assumed to be finite. Following the notation in [3], we construct a probability space $(\Omega, \mathcal{F}, \mathbb{P})$, where \mathcal{F} represents the σ -algebra of events on Ω and \mathbb{P} is a probability measure defined on \mathcal{F} satisfying standard measure-theoretic properties. Let $X : \Omega \rightarrow \mathbb{R}$ be a random variable representing our RA metric for any given scenario. For each generator $g \in \mathcal{G}$, let $x_g \in \mathbb{R}_+$ denote its installed capacity. In the absence of storage, and assuming that generation resources have no intertemporal operating constraints, we define

$$A_{g\tau\omega} : \mathcal{T} \times \Omega \rightarrow [0, 1]$$

as a stochastic process representing generator g 's availability, where $A_{g\tau\omega}$ denotes its realization in hour τ of scenario ω . Then, the total available capacity is stochastic processes on $\mathcal{T} \times \Omega \rightarrow \mathbb{R}_+$, defined as

$$\hat{x}_{\tau\omega} = \sum_{g \in \mathcal{G}} x_g A_{g\tau\omega}.$$

The system load profile is assumed to be sampled from a set of representative scenarios, with $L_{\tau\omega}$ denoting load in hour τ of scenario ω . For notational compactness, we define the vectors of hourly values within scenario ω as

$$\hat{x}_{\omega} := (\hat{x}_{\tau\omega})_{\tau \in \mathcal{T}}, \quad \mathbf{L}_{\omega} := (L_{\tau\omega})_{\tau \in \mathcal{T}},$$

representing total available capacity and system load, respectively.

B. Resource Adequacy Metrics

For semantic clarity, we distinguish three related but distinct concepts: the *RA metric*, the *risk measure*, and the *reliability standard*. The RA metric specifies how shortage events are quantified and aggregated within a single assessment period, such as Unserved Energy (UE), Loss of Load Hours (LOLH), and Loss of Load Days (LOLD). The risk measure defines how these per-scenario outcomes are aggregated across multiple stochastic realizations (e.g., expectation or percentile). Finally, the reliability standard specifies the target or benchmark value of the risk measure that the system is expected to satisfy, such as the ‘one day in ten years’ LOLD criterion commonly used in North America through the 1960s [11].

We first define the RA metric for each scenario ω as a functional

$$M : \mathbb{R}_+^{|\mathcal{T}|} \times \mathbb{R}_+^{|\mathcal{T}|} \rightarrow \mathbb{R}_+, \quad M(\hat{x}_{\omega}, \mathbf{L}_{\omega}),$$

which aggregates unserved load over time according to the chosen reliability measure. Examples include:

$$\begin{aligned} M_{\text{LOLH}}(\hat{x}_{\omega}, \mathbf{L}_{\omega}) &= \sum_{\tau \in \mathcal{T}} \mathbb{1}\{(L_{\tau\omega} - \hat{x}_{\tau\omega}) > 0\}, \\ M_{\text{LOLD}}(\hat{x}_{\omega}, \mathbf{L}_{\omega}) &= \sum_{d \in \mathcal{D}} \mathbb{1}\left\{\max_{\tau \in \mathcal{T}_d} (L_{\tau\omega} - \hat{x}_{\tau\omega}) > 0\right\}, \\ M_{\text{UE}}(\hat{x}_{\omega}, \mathbf{L}_{\omega}) &= \sum_{\tau \in \mathcal{T}} (L_{\tau\omega} - \hat{x}_{\tau\omega})_+, \end{aligned}$$

where $(\cdot)_+ := \max\{\cdot, 0\}$.

The system-level RA measure is defined by aggregating the per-scenario metric across the probability space:

$$\mathcal{M}(\hat{x}, \mathbf{L}) := \Phi_{\omega}[M(\hat{x}_{\omega}, \mathbf{L}_{\omega})],$$

where $\Phi_{\omega}[\cdot]$ is a risk operator. Common choices include the expectation $\Phi_{\omega}[Y] = \mathbb{E}_{\omega}[Y]$, or a tail-risk measure such as the conditional value-at-risk (CVaR).

III. GRADIENT-BASED CAPACITY ACCREDITATION METHODS

A. Assumptions

Capacity accreditation is performed relative to a baseline system configuration. In practice, the system operator first estimates the baseline system's Installed Capacity Requirement (ICR) prior to accreditation using historical information, planned retirements, and policy-driven assumptions (e.g., renewable portfolio targets). Throughout this paper, we let \hat{x} denote the operator's baseline estimate of available capacity trajectories used in the accreditation study. This baseline plays a central role in marginal-based accreditation methods, as both ELCC and MRI quantify reliability impacts relative to this reference system. We adopt the notation of Section II and impose the following assumptions.

Assumption 1 (Baseline Shortfall and Shortfall Dependence): Assume the baseline system is not perfectly adequate,

i.e., $\mathcal{M}(\hat{\mathbf{x}}, \mathbf{L}) > 0$, and that there exists a functional $\widetilde{\mathcal{M}}$ such that, for any pair of trajectories $(\hat{\mathbf{x}}, \mathbf{L})$,

$$\mathcal{M}(\hat{\mathbf{x}}, \mathbf{L}) = \widetilde{\mathcal{M}}(\mathbf{L} - \hat{\mathbf{x}}). \quad (1)$$

Equivalently, for any scalar $c \in \mathbb{R}$,

$$\mathcal{M}(\hat{\mathbf{x}} + c\mathbf{1}, \mathbf{L} + c\mathbf{1}) = \mathcal{M}(\hat{\mathbf{x}}, \mathbf{L}). \quad (2)$$

This assumption holds for standard RA metrics combined with common risk operators (e.g., expectation or quantiles), since these measures depend only on shortfalls.

Assumption 2 (Monotonicity and Continuity): \mathcal{M} is non-increasing in $\hat{\mathbf{x}}$ and nondecreasing in \mathbf{L} (componentwise), and is continuous in both arguments.

Assumption 2 also holds for non-storage resources under standard RA metrics with common risk operators. For storage resources, however, monotonicity must be verified with respect to the assumed dispatch policy, as the effective contribution of storage depends on intertemporal operating decisions [19].

Assumption 3 (Directional Differentiability at the Baseline): At the baseline $(\hat{\mathbf{x}}, \mathbf{L})$, the risk measure \mathcal{M} admits (Gâteaux) directional derivatives in the directions relevant for capacity accreditation. Specifically, for any direction $\mathbf{v} \in \mathbb{R}_+^{|\mathcal{T}|}$ of interest,

$$\partial_{\hat{\mathbf{x}}} \mathcal{M}[\mathbf{v}] := \frac{d}{d\epsilon} \bigg|_{\epsilon=0} \mathcal{M}(\hat{\mathbf{x}} + \epsilon\mathbf{v}, \mathbf{L}) \quad (3)$$

exists. Here, \mathbf{v} represents a capacity-availability perturbation associated with a marginal change in a single resource, a resource class, or a colocated portfolio (e.g., $v_\tau = A_{g\tau}$ for a candidate unit g). We further assume that the baseline evaluation point is *regular* in the sense that it does not coincide with a kink of the underlying piecewise-linear mapping; in particular, this is typically satisfied when the baseline system exhibits nonzero shortfall under the chosen metric.

In this paper, we primarily focus on EUE, for which \mathcal{M} is piecewise linear in $\hat{\mathbf{x}}$ and may fail to be differentiable *only* at turning points where marginal capacity does change the set of shortage hours [20]. Since accreditation evaluates derivatives at a fixed baseline and along specific directions, assuming regularity at the baseline is mild in practice. For other metrics such as LOLD, which involve indicator functions and maxima, analogous results continue to hold when $\partial_{\hat{\mathbf{x}}} \mathcal{M}$ is interpreted as an appropriate subgradient or when limits are taken along regular (non-degenerate) points.

B. Effective Load Carrying Capability (ELCC)

The ELCC of a candidate unit quantifies the largest constant load L_c that can be added while maintaining the same system-level reliability after adding the unit.

Definition 1 (Marginal ELCC): Let the candidate unit have additional nameplate capacity $\Delta x > 0$ and scenario-wise availability $\mathbf{A}_{g,\omega} = (A_{g\tau\omega})_{\tau \in \mathcal{T}}$. The *largest* L_c meeting

$$\mathcal{M}(\hat{\mathbf{x}} + \Delta x \mathbf{A}_g, \mathbf{L} + L_c \mathbf{1}) = \mathcal{M}(\hat{\mathbf{x}}, \mathbf{L}) \quad (4)$$

is defined as the value ELCC. Then, the associated *ELCC Capacity Accreditation* is the fraction of nameplate credited:

$$\alpha_g^{\text{ELCC}} := \frac{L_c}{\Delta x} \in [0, 1]. \quad (5)$$

Proposition 1 (Equivalent ELCC formulation): Under Assumption 1, (4) is equivalent to

$$\mathcal{M}(\hat{\mathbf{x}} + \Delta x \mathbf{A}_g, \mathbf{L}) = \mathcal{M}(\hat{\mathbf{x}} + L_c \mathbf{1}, \mathbf{L}), \quad (6)$$

where $\hat{\mathbf{x}} + L_c \mathbf{1}$ corresponds to adding L_c MW of a resource uniformly available across all periods and without outage.

Remark: The value L_c defined by (6) is often referred to as the marginal *Equivalent Firm Capacity* (EFC). Under Assumption 1, marginal EFC is numerically equivalent to marginal ELCC *locally*, although the two concepts differ in physical interpretation: ELCC is framed as an equivalent load increase, whereas EFC is framed as an equivalent addition of perfectly firm capacity [21].

Proposition 2 (Existence and Uniqueness of L_c for EUE): Fix $\Delta x > 0$ and let \mathcal{M} be the EUE-based risk measure. Under Assumptions 1, 2, and 3, there exists a unique $L_c \geq 0$ satisfying (4) or (6).

Proof. Consider the function

$$\phi(c) = \mathcal{M}(\hat{\mathbf{x}} + c\mathbf{1}, \mathbf{L}) - \mathcal{M}(\hat{\mathbf{x}} + \Delta x \mathbf{A}_g, \mathbf{L}), \quad c \geq 0.$$

By Assumption 2, ϕ is continuous and nonincreasing in c (adding firm capacity cannot increase EUE). Moreover, $\phi(0) \geq 0$ since $\Delta x \mathbf{A}_g \geq \mathbf{0}$ implies $\mathcal{M}(\hat{\mathbf{x}}, \mathbf{L}) \geq \mathcal{M}(\hat{\mathbf{x}} + \Delta x \mathbf{A}_g, \mathbf{L})$. As $c \rightarrow +\infty$, EUE vanishes, so $\mathcal{M}(\hat{\mathbf{x}} + c\mathbf{1}, \mathbf{L}) \rightarrow 0$ and hence $\phi(c) \rightarrow -\mathcal{M}(\hat{\mathbf{x}} + \Delta x \mathbf{A}_g, \mathbf{L}) < 0$, where strict negativity uses Assumption 1 and $\Delta x < \infty$. Therefore, by the intermediate value theorem, there exists $L_c \geq 0$ such that $\phi(L_c) = 0$, which is exactly (6).

For uniqueness, Assumption 3 implies that ϕ has directional derivative

$$\phi'(c) = \partial_{\hat{\mathbf{x}}} \mathcal{M}[\mathbf{1}] \bigg|_{(\hat{\mathbf{x}} + c\mathbf{1}, \mathbf{L})}.$$

For the EUE metric, $\partial_{\hat{\mathbf{x}}} \mathcal{M}[\mathbf{1}] < 0$ whenever there is positive probability of shortfall, so ϕ is strictly decreasing on the relevant range. Hence $\phi(c) = 0$ has at most one solution, and L_c is unique. \square

Proposition 3 (First-order ELCC response): Assume \mathcal{M} is the EUE-based risk measure. Under Assumptions 1 and 3, as $\Delta x \rightarrow 0$ the ELCC L_c satisfying (6) obeys

$$L_c = \frac{\partial_{\hat{\mathbf{x}}} \mathcal{M}[\mathbf{A}_g]}{\partial_{\hat{\mathbf{x}}} \mathcal{M}[\mathbf{1}]} \Delta x + o(\Delta x), \quad (7)$$

and therefore

$$\alpha_g^{\text{ELCC}} = \frac{L_c}{\Delta x} = \frac{\partial_{\hat{\mathbf{x}}} \mathcal{M}[\mathbf{A}_g]}{\partial_{\hat{\mathbf{x}}} \mathcal{M}[\mathbf{1}]} + o(1). \quad (8)$$

Proof. Using the equivalent ELCC formulation (6), define

$$F(\Delta x, c) := \mathcal{M}(\hat{\mathbf{x}} + \Delta x \mathbf{A}_g, \mathbf{L}) - \mathcal{M}(\hat{\mathbf{x}} + c\mathbf{1}, \mathbf{L}).$$

Then $F(0, 0) = 0$ and the ELCC condition is $F(\Delta x, L_c) = 0$. By Assumption 3, the directional derivatives at $(0, 0)$ satisfy

$$\frac{\partial F}{\partial \Delta x} \Big|_{(0,0)} = \partial_{\hat{x}} \mathcal{M}[\mathbf{A}_g], \quad \frac{\partial F}{\partial c} \Big|_{(0,0)} = -\partial_{\hat{x}} \mathcal{M}[\mathbf{1}].$$

A first-order expansion around $(0, 0)$ gives

$$0 = F(\Delta x, L_c) = \partial_{\hat{x}} \mathcal{M}[\mathbf{A}_g] \Delta x - \partial_{\hat{x}} \mathcal{M}[\mathbf{1}] L_c + o(\Delta x + L_c),$$

which rearranges to

$$L_c = \frac{\partial_{\hat{x}} \mathcal{M}[\mathbf{A}_g]}{\partial_{\hat{x}} \mathcal{M}[\mathbf{1}]} \Delta x + o(\Delta x).$$

Dividing by Δx yields the expression for α_g^{ELCC} . \square

C. Marginal Reliability Impact (MRI)

The MRI formalizes the directional sensitivity of the risk measure to an incremental addition of resource g .

Definition 2 (MRI): For $\Delta x > 0$, define the finite-difference MRI of g at $(\hat{\mathbf{x}}, \mathbf{L})$ by

$$\text{MRI}_g(\Delta x) := \frac{\mathcal{M}(\hat{\mathbf{x}} + \Delta x \mathbf{A}_g, \mathbf{L}) - \mathcal{M}(\hat{\mathbf{x}}, \mathbf{L})}{\Delta x}. \quad (9)$$

Based on Assumption 3, the MRI can be formulated as:

$$\text{MRI}_g := \partial_{\hat{x}} \mathcal{M}[\mathbf{A}_g] = \lim_{\Delta x \rightarrow 0} \text{MRI}_g(\Delta x). \quad (10)$$

Definition 3 (Perfect Resource): A perfect resource delivers one unit in every hour, i.e. its availability trajectory is $\mathbf{1}$. Its marginal MRI is $\text{MRI}_{\text{perf}} := \partial_{\hat{x}} \mathcal{M}[\mathbf{1}]$.

Definition 4 (MRI-based Capacity Accreditation): The MRI-based accreditation factor of g is defined by normalizing its marginal impact by the perfect resource:

$$\alpha_g^{\text{MRI}} := \frac{\text{MRI}_g}{\text{MRI}_{\text{perf}}} = \frac{\partial_{\hat{x}} \mathcal{M}[\mathbf{A}_g]}{\partial_{\hat{x}} \mathcal{M}[\mathbf{1}]} \quad (11)$$

D. Equivalence of Capacity Accreditation

We now state and prove the local equivalence between ELCC- and MRI-based capacity accreditation, a relationship that has also been discussed informally in [22].

Proposition 4 (Equivalence of ELCC and MRI Accreditation): Assume \mathcal{M} is the EUE-based risk measure. Under Assumptions 1, 2, and 3, the marginal ELCC accreditation factor equals the MRI-based accreditation factor:

$$\alpha_g^{\text{ELCC}} = \alpha_g^{\text{MRI}} = \frac{\partial_{\hat{x}} \mathcal{M}[\mathbf{A}_g]}{\partial_{\hat{x}} \mathcal{M}[\mathbf{1}]}.$$

Proof. Taking $\Delta x \rightarrow 0$ and applying Proposition 3 and Definition 4 yields the claim. \square

Remark: Since most practical capacity accreditation exercises rely on finite (non-infinitesimal) perturbations, the resulting accreditation values may exhibit slight dependence on the chosen perturbation size [6].

IV. INFINITESIMAL PERTURBATION ANALYSIS

Gradient-based capacity accreditation relies on the existence of a well-defined *infinitesimal* sensitivity of the risk measure $\mathcal{M}(\hat{\mathbf{x}}, \mathbf{L})$ with respect to available capacity. This section presents the infinitesimal perturbation analysis framework for characterizing and interpreting such sensitivities through unbiased pathwise derivatives.

A. Infinitesimal Perturbation Analysis

In a stochastic simulation setting, the key theoretical question is whether this gradient can be interpreted as the expectation of a scenario-wise (sample-path) derivative—i.e., whether differentiation can be interchanged with the risk operator (here, expectation). This interchange is the foundation of *infinitesimal perturbation analysis* (IPA) and provides a rigorous meaning for “marginal reliability impact” as a true derivative rather than a finite-difference artifact [16], [17].

Definition 5 (Infinitesimal Perturbation Analysis (IPA)) [16], [17]: Let $F(\hat{\mathbf{x}}, \mathbf{L}; \omega)$ denote a scenario-wise performance measure (e.g., unserved energy), and let the risk measure be $\mathcal{M}(\hat{\mathbf{x}}, \mathbf{L}) = \mathbb{E}_\omega[F(\hat{\mathbf{x}}, \mathbf{L}; \omega)]$. IPA refers to estimating a directional derivative of \mathcal{M} using the corresponding *pathwise* directional derivative of F , i.e.,

$$\partial_{\hat{x}} \mathcal{M}[\mathbf{v}] = \partial_{\hat{x}} [\mathbb{E}_\omega F[\mathbf{v}]] = \mathbb{E}_\omega [\partial_{\hat{x}} F[\mathbf{v}]],$$

whenever the interchange of differentiation and expectation is valid. In this case, $\partial_{\hat{x}} F[\mathbf{v}]$ provides an unbiased single-scenario contribution to the gradient, enabling step-size-free sensitivity estimation.

Proposition 5 (IPA for EUE): Consider the EUE setting where the scenario-wise unserved energy is

$$\mathcal{M}(\hat{\mathbf{x}}, \mathbf{L}) := \mathbb{E}_\omega[F(\hat{\mathbf{x}}, \mathbf{L}; \omega)] = \mathbb{E}_\omega \sum_{\tau \in \mathcal{T}} (L_{\tau\omega} - \hat{x}_{\tau\omega})_+ \quad (12)$$

Under Assumptions 1, 2, and 3, the following mild regularity conditions hold: (i) $\mathbb{P}\{L_{\tau\omega} = \hat{x}_{\tau\omega}\} = 0$ for all $\tau \in \mathcal{T}$, and (ii) $F(\hat{\mathbf{x}}, \mathbf{L}; \omega)$ is integrable and uniformly Lipschitz in $\hat{\mathbf{x}}$ in a neighborhood of the baseline. Consequently, differentiation and expectation can be interchanged. In particular, \mathcal{M} admits a directional derivative in any direction $\mathbf{v} \in \mathbb{R}^{|\mathcal{T}|}$ and

$$\partial_{\hat{x}} \mathcal{M}[\mathbf{v}] = \mathbb{E}_\omega[\partial_{\hat{x}} F[\mathbf{v}]] = -\mathbb{E}_\omega \left[\sum_{\tau \in \mathcal{T}} v_\tau \mathbb{1}\{L_{\tau\omega} > \hat{x}_{\tau\omega}\} \right]. \quad (13)$$

Proof. For each τ , the mapping $\hat{x}_{\tau\omega} \mapsto (L_{\tau\omega} - \hat{x}_{\tau\omega})_+$ is piecewise linear with slope -1 when $L_{\tau\omega} > \hat{x}_{\tau\omega}$ and slope 0 otherwise. Under (i), the kink event occurs with probability zero, so the pathwise derivative exists almost surely. Condition (ii) supplies an integrable dominating bound, allowing differentiation and expectation to be interchanged via dominated convergence, which yields (13). \square

Proposition 5 provides two key interpretations for gradient-based capacity accreditation. First, while calculating Loss of Load Probability (LOLP)-weighted average availability has long been suggested as a simpler heuristic for ELCC, but

never formally justified [23]. We formalize that the “marginal impact” of capacity is a well-defined sensitivity of the *expected* shortfall, rather than a numerical artifact arising from a particular perturbation size.

Second, as illustrated in Fig. 1, (13) yields an explicit pathwise estimator for this sensitivity: the directional derivative corresponds to the expected *shortage-weighted* availability along a given direction \mathbf{v} . Unlike finite-difference approaches, which require repeated simulations with different capacity increments and are sensitive to step-size selection, the IPA approach computes gradients directly by aggregating pathwise contributions from a single simulation run.

In particular, choosing $\mathbf{v} = \mathbf{A}_g$ yields the gradient direction associated with resource g , while choosing $\mathbf{v} = \mathbf{1}$ recovers the perfect-resource benchmark defined in Definition 3. As a result, IPA enables gradient-based capacity accreditation for *all* non-storage resources to be obtained from *one* resource adequacy simulation, substantially reducing computational burden while maintaining high estimation accuracy. For storage resources, pathwise sensitivity becomes more complex, as it depends on the full period profile and the assumed dispatch policy.

B. Pathwise Sensitivity

Proposition 5 implies that, under an EU-based risk measure, marginal capacity value is determined by *coincidence with scarcity*. Define the baseline scarcity indicator $S_{\tau\omega} := \mathbb{1}\{L_{\tau\omega} > \hat{x}_{\tau\omega}\}$. Then the directional derivative can be expressed as

$$\partial_{\hat{x}} \mathcal{M}[\mathbf{v}] = -\mathbb{E}_{\omega} \left[\sum_{\tau \in \mathcal{T}} v_{\tau} S_{\tau\omega} \right]. \quad (14)$$

Equation (14) provides a direct interpretation: an incremental unit of capacity in period τ reduces EU only in those scenarios and hours in which the system is already short.

While IPA offers substantial computational convenience for accrediting individual resources, evaluating the *joint* contribution of portfolios that include intertemporal storage resources requires additional care when interpreting (14). For conventional generators or renewables, the perturbation direction \mathbf{v} can often be treated as exogenous (e.g., $\mathbf{v} = \mathbf{A}_g$). In contrast, the net injection profile of storage is induced by operational decisions (charging/discharging subject to state-of-charge constraints) and therefore depends on an operating policy and on scenario history. It is thus more appropriate to represent the perturbation direction as $\mathbf{v}(\pi)$ for a specified policy π , potentially scenario-dependent, rather than as a fixed time series [24]. Some optimization-based formulations can be useful for evaluating the MRI of storage resources by explicitly modeling intertemporal operating decisions and state-of-charge constraints [19].

This observation also clarifies why the accreditation of a combined resource is generally not additive. When storage is paired with *any* other resources—*whether renewable, gas, or nuclear*—its feasible and optimal actions are coupled to the paired resource’s availability history (through charging opportunities) and to system scarcity conditions. As a result,

the marginal contribution of the combined portfolio cannot, in general, be recovered by separately accrediting each component and summing the resulting credits. The interaction arises from the fact that the storage-induced direction $\mathbf{v}(\pi)$ is not invariant to the presence or temporal pattern of the paired resource; instead, the portfolio modifies the effective coincidence with scarcity in (14) through an endogenous reshaping of injections over time.

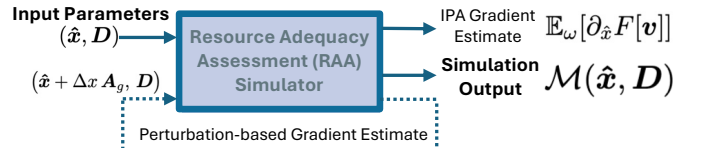


Fig. 1: Comparison between IPA-based direct gradient estimation and perturbation-based gradient estimation.

V. PERTURBATION-BASED COMPUTATION AND PRACTICAL IMPLICATIONS

While IPA (13) provides a direct and efficient approach for gradient computation, its application typically requires access to internal information from the RAA simulator, which may not always be available in practice. In addition, evaluating joint resource portfolios can pose further challenges. As compared in Fig. 1, industry implementations commonly rely on repeated RAA simulations using perturbation-based methods. This section discusses practical considerations in such simulations and highlights the fundamental computational differences between ELCC- and MRI-based capacity accreditation.

A. Sample Size in Resource Adequacy Assessment

Determining the appropriate sample size of MC simulation for a probabilistic resource adequacy assessment requires balancing computational effort with the desired statistical accuracy of the study outcomes. Define the i.i.d. random variable $Z = \mathcal{M}(\hat{x}, \mathbf{L})$. Given n simulated scenarios Z_1, \dots, Z_n under representatively sampled random operating conditions, the MC estimator is $\bar{Z}_n = \frac{1}{n} \sum_{i=1}^n Z_i$. By the Central Limit Theorem (CLT), for large n the estimator \bar{Z}_n is approximately normally distributed with variance s^2/n , where s^2 is the sample variance of the observations.

While increasing n helps achieve a target confidence interval, the nonnegative structure of RA metrics introduces important limitations. Reliability shortfalls are rare events, so most simulated scenarios yield “all-zero” outcomes with no unserved energy. Some alternative approaches, such as the *zero-shortfall sample* (CLT+) method and *Bayesian prior*-based estimation, were proposed recently to improve inference accuracy [13].

B. Step Size in Perturbation-based Gradient Estimation

Both ELCC and MRI ultimately require estimating how the risk measure changes under a small perturbation to available capacity. When gradients are approximated by finite differences, one must choose a *perturbation step size* (e.g., a small MW change), which creates a bias-variance tradeoff.

Step Size Selection: Let $\delta > 0$ be a small capacity perturbation. A central difference estimator is given by:

$$\widehat{\text{MRI}}_g(\delta) = \frac{\mathcal{M}(\hat{\mathbf{x}} + \delta \mathbf{A}_g, \mathbf{L}) - \mathcal{M}(\hat{\mathbf{x}} - \delta \mathbf{A}_g, \mathbf{L})}{2\delta}. \quad (15)$$

The choice of δ involves a fundamental bias–variance trade-off. If δ is too large, the finite-difference estimator approximates a secant rather than the desired tangent, introducing truncation bias. Conversely, if δ is too small, the difference in the numerator becomes dominated by Monte Carlo variability, inflating variance through cancellation error. To mitigate this effect, industry implementations typically rely on *Common Random Numbers* (CRN), i.e., using identical random-number streams (or equivalently, the same set of sampled scenarios) for both the baseline and perturbed simulations. This practice induces positive correlation between the paired outputs, which reduces the variance of the difference estimator relative to using independent simulations [25]. In practice, fixing the number of samples and reusing the same scenarios for baseline and perturbed runs serves a similar purpose by ensuring that differences between runs are attributable primarily to the perturbation rather than sampling variability.

From a statistical perspective, the residual *simulation noise* reflects the uncertainty inherent in Monte Carlo estimates of reliability metrics. In resource adequacy studies, this uncertainty is commonly quantified using the relative standard error (RSE), defined as the ratio of the estimator's standard deviation to its mean. Components of the estimated change that are on the order of, or smaller than, the RSE are effectively indistinguishable from noise. For example, any part of the result smaller than RSE would be simulation noise in the ISO New England practice.

Theoretically, for central finite-difference gradient estimators under independent simulation noise, minimizing mean-square error leads to an optimal step size that scales with $N^{-1/6}$, reflecting a balance between squared bias $O(\delta^4)$ and variance $O(1/(N\delta^2))$ [26]. While CRN and large fixed sample sizes can substantially reduce variance and allow for smaller δ , a practical lower bound remains due to the discrete nature of reliability outcomes. If δ is smaller than the effective “distance” to the next state change, such as the increment required to trigger an additional shortage hour, then the finite difference $\mathcal{M}(+\delta) - \mathcal{M}(-\delta)$ may evaluate to zero for certain metrics, yielding a vanishing gradient estimate. Consequently, practitioners typically select the smallest perturbation size that produces changes exceeding the RSE threshold, thereby preserving numerical sensitivity while controlling bias.

In industry implementations, different system operators adopt perturbation strategies that reflect both computational considerations and modeling practices. PJM Interconnection computes marginal ELCC using 100 MW increments for both resource-class and unit-specific studies [27]. ISO New England has proposed smaller perturbations for MRI-based calculations, applying a 0.5 MW perturbation to resource capacities while constructing demand curves by sweeping system capacity in 10 MW increments around the ICR [28]. Through extensive testing, the New York ISO has determined that MRI provides a sufficiently accurate approximation of

ELCC at a fraction of the computational cost, and therefore currently applies MRI using a 100 MW perturbation step size in its capacity accreditation framework [29].

C. Fundamental Difference Between ELCC and MRI-based Capacity Accreditation

The MRI ratio is attractive computationally because it avoids solving the implicit equation for L_c , but requires only two directional sensitivities, which can be estimated by finite differences within a single simulation run.

Different from the MRI method, the ELCC requires an iterative search procedure to find the equivalent load-carrying capacity. Recall that the ELCC L_c is the root of the nonlinear equation:

$$g(c) = \mathcal{M}(\hat{\mathbf{x}} + \Delta x \mathbf{A}_g, \mathbf{L} + c \mathbf{1}) - \mathcal{M}(\hat{\mathbf{x}}, \mathbf{L}). \quad (16)$$

Solving this equation for $c = L_c$ creates a significant computational burden characterized by the following factors:

1) *Iterative Root-Finding*: Unlike the MRI, which is a local linear approximation evaluated at the current system state, ELCC seeks a specific point on the reliability surface where risk is invariant. Since the risk function \mathcal{M} does not have a closed-form inverse, L_c must be found using numerical root-finding algorithms, typically a bisection search method.

2) *Nested Simulation Loops*: Fig. 2 illustrates the computation process of perturbation-based ELCC and MRI capacity accreditation. The computational cost of ELCC is multiplicative. Let C_{sim} be the cost of one resource adequacy simulation (e.g., a full sequential Monte Carlo year). Assuming the baseline system and perfect increment capacity scenarios have been simulated, then for each study resource, we have

- **MRI Complexity:** The cost is $\approx C_{\text{sim}}$. All marginal accreditation factors can be computed in a single run.
- **ELCC Complexity:** If the root-finding algorithm requires k iterations to converge to a specified tolerance (e.g., ϵ_{MW}), the cost for a *single* resource is $k \times C_{\text{sim}}$.

In practice, k often ranges from 5 to 15 iterations depending on the convexity of the risk curve and the required precision.

3) *Accelerated Root-Finding via Gradient Methods*: Standard industry tools typically employ *bisection search* (bilateral search) to solve the ELCC equation $g(c) = 0$. While bisection is robust against non-smoothness, it converges linearly, halving the uncertainty interval at each step. To reduce the computational burden, some gradient-based methods might accelerate the computing process.

The common root-finding process can be driven by *Newton's Method*. The update rule is given by:

$$c_{k+1} = c_k - \frac{g(c_k)}{g'(c_k)}. \quad (17)$$

where the derivative $g'(c_k)$ represents the sensitivity of system reliability to a shift in firm load.

However, in many practical implementations, computing the gradient $g'(c_k)$ at each iteration is either computationally expensive or not directly available, as it effectively requires a full MRI evaluation. In this paper, we therefore employ the *secant method*, which retains the convergence acceleration benefits

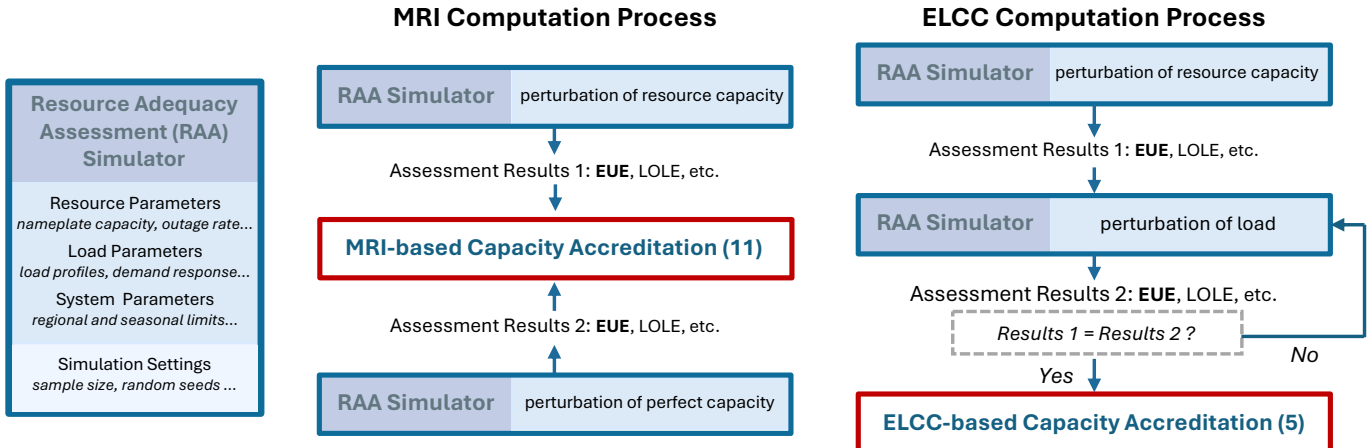


Fig. 2: Computation Process of *Perturbation-based* ELCC and MRI Capacity Accreditation

of gradient-based root finding while avoiding explicit gradient computations. This quasi-Newton approach approximates the derivative using the history of function evaluations from the two previous iterations, c_k and c_{k-1} :

$$c_{k+1} = c_k - g(c_k) \frac{c_k - c_{k-1}}{g(c_k) - g(c_{k-1})}. \quad (18)$$

This method offers a superlinear rate of convergence and is significantly faster than bisection. Crucially, it requires only **one** reliability simulation per iteration (to evaluate $g(c_k)$), as the previous value $g(c_{k-1})$ is cached.

To improve robustness against stochastic noise inherent in Monte Carlo simulations, hybrid root-finding approaches (e.g., *Brent's method*), which combine bisection with secant-type steps for faster convergence, can also be effective. A detailed discussion of these methods is omitted due to space limitations.

VI. NUMERICAL CASE STUDY

A. System Description

The RTS-GMLC reliability test system represents a contemporary generation portfolio with resource characteristics calibrated to real-world data [30]. The system consists of a single region with 153 generators and a total installed capacity of 14,138 MW. The generation mix includes 73 thermal units (coal, gas, oil, and nuclear) totaling 8,126 MW, 20 hydro units totaling 1,000 MW, 56 solar units totaling 2,504 MW, and 4 wind farms totaling 2,508 MW. In addition, the system includes one battery storage resource with a power capacity of 50 MW and an energy duration of 3 hours. The system load profile is uniformly scaled to establish a baseline system reliability level close to the '1-in-10' standard. Under this baseline, the system peak load is 9,502.7 MW, corresponding to a system-wide LOLD of 2.10 hours/year and EU of 394.2 MWh/year.

This study uses the Julia-based open-source simulator PRAS [10] with an hourly temporal resolution and a resource capacity resolution of 0.1 MW. For non-intermittent resources, scenarios are sampled from a distribution function representing the outage rate, while for intermittent resources, scenarios

are sampled from historical data. To ensure high statistical accuracy, we employ 1,000,000 Monte Carlo samples for each RA assessment. All simulations are executed on the Harvard Research Computing cluster: each RA assessment utilizes 2 Intel Xeon Sapphire Rapids CPUs (112 cores total) with 256 GB of memory. The inter-regional transmission constraints are not the focus of this paper and are therefore excluded from the analysis.

B. Capacity Accreditation Factors and Computation Time

We first select 9 representative generators for gradient-based capacity accreditation, including gas combined-cycle (CC), gas combustion turbine (CT), coal, nuclear, oil, hydro, wind, PV, and battery storage. The unit-level results facilitate a direct methodological comparison. In practice, capacity accreditation is often assigned at the resource-class level based on a weighted average of individual generator accreditation.

For the three perturbation-based methods, i.e. ELCC with bisection, ELCC with secant search, and perturbation-based MRI, we apply a 10 MW perturbation relative to each resource's nameplate capacity. For renewable resources, the perturbation is applied proportionally to the output profile, while for storage resources, both power and energy capacities are scaled proportionally to preserve duration. In addition, we apply the IPA-based approach to directly compute MRI for non-storage resources, which estimates gradients without requiring repeated perturbation simulations.

TABLE I: Comparison of Capacity Accreditation Factors

Gen ID	ELCC (Bisection)	ELCC (Secant)	MRI (Perturb)	MRI (IPA)	FOR
107 Gas CC	0.84	0.84	0.84	0.84	3.3%
113 Gas CT	0.96	0.96	0.96	0.96	3.1%
115 Coal	0.90	0.91	0.91	0.91	4.0%
121 Nuclear	0.47	0.48	0.48	0.49	12.0%
101 Oil CT*	0.90	0.89	0.89	0.89	10.0%
322 Hydro	0.76	0.75	0.76	0.75	–
122 Wind	0.09	0.08	0.09	0.08	–
215 PV	0.15	0.16	0.16	0.15	–
313 Storage	0.78	0.80	0.81	–	–

*small unit size (20MW)

As shown in Table I, despite differences in numerical implementation, the resulting capacity accreditation factors are highly consistent across all methods. These results empirically validate the theoretical equivalence between ELCC and MRI and confirm the correctness of the IPA-based direct gradient computation approach.

Table II compares the computational performance of the 4 accreditation methods. To quantify the computational burden, we estimate the total number of RAA runs required for the full system as $1 + N_g N_p$. This metric accounts for a single baseline system simulation (the “1”) plus the individual evaluations required for each of the N_g generators, scaled by the average number of perturbations per resource (N_p).

TABLE II: Average computation time per generator (seconds), average perturbation evaluations per resource (N_p), and implied total number of RAA runs for whole system.

Method	Avg. Time (per generator)	Avg. # of Perturb. (N_p)	Total # of RAA
ELCC (Bisection)	452.8	≈ 7	$1 + N_g N_p$
ELCC (Secant)	307.5	≈ 3.7	$1 + N_g N_p$
MRI (Perturb)	65.7	1	$1 + N_g N_p$
MRI (IPA)	0.4*	0	1

* Calculated by dividing the time of a single IPA run by N_g , since one run provides gradients for *all* 153 generator in RTS-GMLC system.

The MRI-based approach is substantially faster than ELCC. Among perturbation-based methods, MRI achieves an order-of-magnitude speedup relative to bisection-based ELCC. This efficiency arises because MRI requires only one perturbation per resource ($N_p = 1$) to estimate capacity factors from marginal sensitivities, whereas ELCC requires multiple iterative simulations ($N_p \approx 7$) to solve an implicit reliability-equivalence condition. Within the ELCC framework, the secant method proposed in this paper improves upon standard bisection. By exploiting gradient information to accelerate the root-finding process, the secant method reduces the required perturbations to $N_p \approx 3.7$, yielding a computation time reduction of approximately 32%.

Finally, the IPA-based gradient estimation method provides the most efficient solution. It requires only a single simulation run (Total # of RAA = 1) to compute MRI for *all* non-storage resources simultaneously, effectively decoupling computational cost from the system size N_g . For the RTS-GMLC system with 153 generators, we report the effective per-resource time by dividing the single IPA runtime by N_g . As shown in Table II, this results in an approximately **1000**× speedup relative to the conventional bisection-based ELCC method.

C. Perturbation Step Size

The choice of perturbation step size (Δx) plays a critical role in both ELCC and MRI calculations. Figure 3 compares capacity accreditation factors computed using 3 methods for a range of perturbation sizes from 1 MW to 30 MW. Results are shown for 3 representative generators with distinct characteristics: a 55 MW Gas CT, a 400 MW Nuclear, and a PV plant with 115 MW peak output.

Across all cases, MRI and secant-based ELCC exhibit greater robustness to the choice of perturbation size, producing relatively stable accreditation factors over a wide range of Δx . In contrast, bisection-based ELCC shows higher sensitivity to step size, particularly for small perturbations, reflecting its reliance on repeated evaluations of noisy reliability estimates. This sensitivity is also influenced by the numerical resolution of the underlying simulator. In this study, a capacity resolution of 0.1 MW is used, implying that perturbations smaller than a few megawatts may fail to induce discernible changes in system states and thus amplify numerical noise in finite-difference estimates.

D. Perturbation Direction

In addition to perturbation step size, gradient-based accreditation depends critically on the *perturbation direction*, i.e., how incremental capacity is represented within the resource adequacy model. For conventional generators and variable renewables, the perturbation direction can typically be treated as exogenous and proportional to an availability trajectory, so the marginal impact is governed by the coincidence between the added availability and scarcity periods. For storage resources, however, the effective net-injection profile is endogenously determined by intertemporal operating decisions and state-of-charge constraints. This motivates representing storage perturbations as policy-induced directions $v(\pi)$ rather than fixed time series, and implies that joint portfolios involving storage need not exhibit additive marginal impacts.

TABLE III: Comparison of EUE and Capacity Accreditation Factors under Different Perturbation Directions

Perturbation Direction	EUE (MWh/year)	Δ EUE (MWh/year)	MRI (Perturb)
5 MW Nuclear	389.00	5.22	0.48
5 MW PV	392.51	1.72	0.16
5 MW Storage	385.51	8.71	0.81
5 MW Nuclear, 5 MW Storage	380.43	13.80	0.65
5 MW PV, 5 MW Storage	383.82	10.40	0.49

Table III illustrates the role of perturbation direction using perturbation-based MRI under several incremental additions. The second column reports the resulting EUE under each perturbation, while the third column reports the corresponding reduction relative to the baseline system. The joint perturbations do not equal the sum of the corresponding standalone effects, indicating that marginal impacts depend on how capacity additions interact temporally rather than on individual resource contributions alone.

This behavior is consistent with the pathwise sensitivity interpretation developed in Section IV. When storage is added, its dispatch reshapes the timing of effective injections by shifting energy across hours, thereby modifying the coincidence between incremental capacity and scarcity periods. Because storage charging opportunities and discharge incentives depend jointly on the availability history of other resources and on system stress conditions, the resulting perturbation direction $v(\pi)$ is scenario-dependent and generally changes when another resource is added simultaneously.

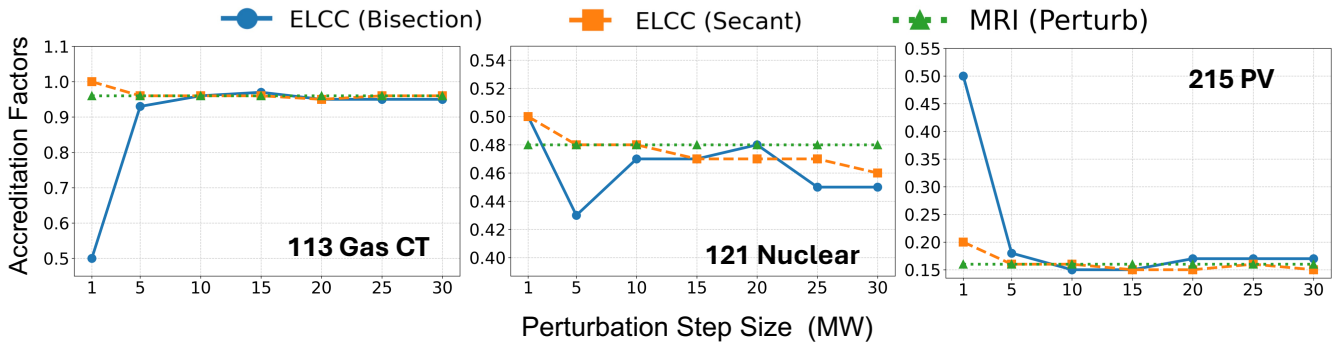


Fig. 3: Effect of perturbation step size on accreditation factors for 3 generators

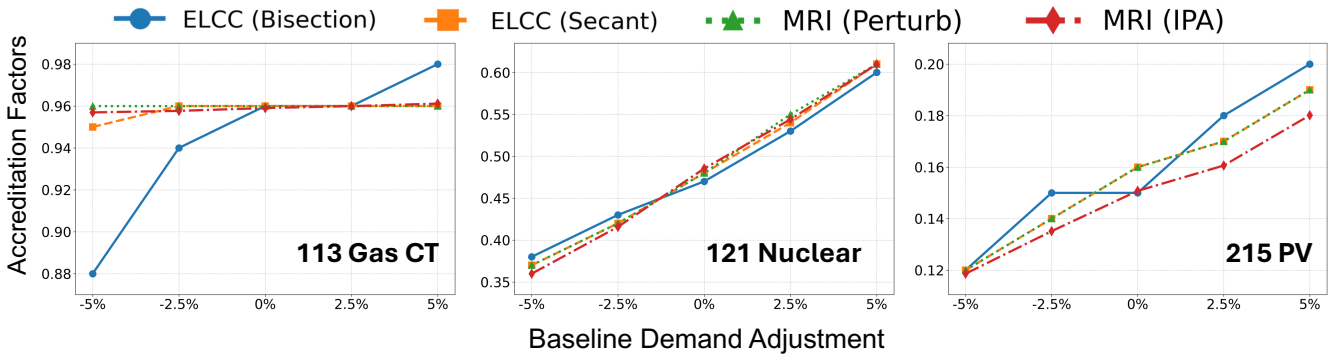


Fig. 4: Effect of baseline load adjustment on accreditation factors for 3 generators

Importantly, this interaction is not specific to renewable resources. Any pairing of storage with another resource can lead to non-additive marginal impacts, which is also categorized as *synergistic* and *antagonistic* combination effects in [31]. Consequently, for storage-inclusive portfolios, defensible accreditation requires explicitly specifying the operating policy used to generate $v(\pi)$, and joint portfolios should be evaluated directly rather than by separately accrediting components and summing their individual credits.

E. Baseline System Reliability Levels

We evaluate the sensitivity of capacity accreditation to system stress by scaling baseline load from -5% to $+5\%$ relative to the reference system. Figure 4 reports results for the same three representative generators. Across all methods, accreditation factors increase monotonically with system stress. As baseline load rises toward the $+5\%$ case, reserve margins shrink and each incremental MW becomes more valuable for maintaining adequacy, resulting in higher accreditation factors. Conversely, under surplus conditions (-5%), accreditation factors flatten and converge, reflecting the diminishing marginal value of capacity when reliability is already high.

Notably, the large nuclear unit consistently exhibits the low accreditation factor despite its 12% physical outage rate, reflecting a “lumpiness” penalty: outages of large units create substantial capacity deficits precisely during high-stress periods. In contrast, the gas CT maintains stable and high accreditation due to its moderate size and low outage rate,

while the PV plant remains constrained by its generation profile, with its contribution capped by the coincidence of solar output and net peak load.

VII. CONCLUSION

This paper develops and applies a gradient-based framework to compare ELCC- and MRI-based capacity accreditation from both theoretical and computational perspectives. Under an EUE-based metric, we establish a local equivalence between marginal ELCC and MRI, while showing that their numerical implementations exhibit fundamentally different computational burdens. In particular, MRI computes accreditation directly from marginal sensitivities within a single Monte Carlo simulation, whereas ELCC relies on iterative root-finding. Among ELCC implementations, secant-based search substantially reduces runtime relative to bisection by exploiting gradient information. We further show that IPA provides a principled and highly efficient mechanism for computing gradient-based accreditation, enabling substantial computational savings when pathwise derivatives are available.

Large-scale numerical results compare the sensitivity of accreditation outcomes to perturbation step size and baseline system reliability level. Overall, MRI is a practical and scalable alternative to ELCC for large-scale accreditation studies, while still needing careful baseline system specification in gradient-based accreditation workflows. Future research will extend IPA-based accreditation to intertemporal resources such as energy storage and integrate the proposed computational framework into capacity market clearing processes.

ACKNOWLEDGMENT

Disclaimer: The views expressed in this paper are solely those of the authors and do not necessarily represent those of ISO New England, PJM Interconnection L.L.C. or its Board of Managers.

REFERENCES

- [1] PJM Interconnection, “Market Design Project Roadmap,” <https://tinyurl.com/pjmcapacity>, 2025.
- [2] ISO New England, “Capacity Auction Reforms Key Project,” <https://www.iso-ne.com/committees/key-projects>, 2025.
- [3] K. X. Zuo, J. C. Macey, and J. Mays, “Revisiting capacity market fundamentals,” *Energy Economics*, p. 108771, 2025.
- [4] H. Nelson, “Practical application of effective load carrying capability (ELCC) in resource adequacy planning,” IEEE Power and Energy Society Resource Adequacy Working Group, Conference Presentation, 2021, presented at RAWG 2021. [Online]. Available: https://cmte.ieee.org/pes-rawg/wp-content/uploads/sites/164/2022/07/Heath_Nelson_NVEnergy_E3_RAWG2021.pdf
- [5] N. Zhang, Y. Yu, C. Fang, Y. Su, and C. Kang, “Power system adequacy with variable resources: A capacity credit perspective,” *IEEE Transactions on Reliability*, vol. 73, no. 1, pp. 53–58, 2023.
- [6] F. Zhao, T. Zheng, D. Schiro, and X. Wang, “A marginal reliability impact based accreditation and capacity market framework,” 2026. [Online]. Available: <https://tinyurl.com/fengmri>
- [7] L. L. Garver, “Effective load carrying capability of generating units,” *IEEE Transactions on Power Apparatus and Systems*, no. 8, pp. 910–919, 1966.
- [8] F. Zhao, T. Zheng, and E. Litvinov, “Constructing demand curves in forward capacity market,” *IEEE Transactions on Power Systems*, vol. 33, no. 1, pp. 525–535, 2017.
- [9] GE Energy Consulting, *Multi-Area Reliability Simulation Program (MARS) User’s Manual*, March 2021.
- [10] G. Stephen, “Probabilistic resource adequacy suite (pras).” National Renewable Energy Laboratory (NREL), Golden, CO, Tech. Rep., 2024.
- [11] G. Stephen, S. H. Tindemans, J. Fazio, C. Dent *et al.*, “Clarifying the interpretation and use of the sole resource adequacy metric,” in 2022 17th International Conference on Probabilistic Methods Applied to Power Systems (PMAPS). IEEE, 2022, pp. 1–4.
- [12] National Academy of Engineering and NERC, “Evolving planning criteria for a sustainable power grid: A workshop report,” Tech. Rep., July 2024. [Online]. Available: <https://tinyurl.com/nercnae>
- [13] G. Stephen and D. Kirschen, “Sample size selection for monte carlo resource adequacy assessment of power systems,” in 2024 18th International Conference on Probabilistic Methods Applied to Power Systems (PMAPS). IEEE, 2024, pp. 1–6.
- [14] C. Singh and A. Lago-Gonzalez, “Reliability modeling of generation systems including unconventional energy sources,” *IEEE Transactions on Power Apparatus and Systems*, vol. 104, no. 5, pp. 1049–1056, 1985.
- [15] Y. Xu and C. Singh, “Power system reliability impact of energy storage integration with intelligent operation strategy,” *IEEE Transactions on smart grid*, vol. 5, no. 2, pp. 1129–1137, 2013.
- [16] M. C. Fu and J.-Q. Hu, *Conditional Monte Carlo: Gradient estimation and optimization applications*. Springer Science, 2012, vol. 392.
- [17] S. Mohamed, M. Rosca, M. Figurnov, and A. Mnih, “Monte carlo gradient estimation in machine learning,” *Journal of Machine Learning Research*, vol. 21, no. 132, pp. 1–62, 2020.
- [18] H. Salehfar and S. Trihadi, “Application of perturbation analysis to sensitivity computations of generating units and system reliability,” *IEEE transactions on power systems*, vol. 13, no. 1, pp. 152–158, 2002.
- [19] Q. Zhang, F. Zhao, T. Zheng, and L. Xie, “Reformulating energy storage capacity accreditation problem with marginal reliability impact,” *arXiv*, 2026.
- [20] S. Zachary, A. Wilson, and C. Dent, “The integration of variable generation and storage into electricity capacity markets,” *The Energy Journal*, vol. 43, no. 4, pp. 231–250, 2022.
- [21] S. Zachary and C. Dent, “Probability theory of capacity value of additional generation,” *Proceedings of the Institution of Mechanical Engineers, part O: Journal of risk and reliability*, vol. 226, no. 1, pp. 33–43, 2012.
- [22] F. Zhao, T. Zheng, D. Schiro, and X. W. Wang, “The MRI-based capacity accreditation: Interpretation and properties,” <https://www.ferc.gov/media/mri-based-capacity-accreditation-interpretation-and-properties>, July 14 2025.
- [23] M. Milligan, “A comparison and case study of capacity credit algorithms for intermittent generators,” National Renewable Energy Lab.(NREL), Golden, CO (United States), Tech. Rep., 1997.
- [24] G. Stephen, T. Joswig-Jones, S. Awara, and D. Kirschen, “Impact of storage dispatch assumptions on resource adequacy and capacity credit,” in 2022 17th International Conference on Probabilistic Methods Applied to Power Systems (PMAPS). IEEE, 2022, pp. 1–6.
- [25] P. Glasserman and D. D. Yao, “Some guidelines and guarantees for common random numbers,” *Management Science*, vol. 38, no. 6, pp. 884–908, 1992.
- [26] M. A. Zazanis and R. Suri, “Convergence rates of finite-difference sensitivity estimates for stochastic systems,” *Operations Research*, vol. 41, no. 4, pp. 694–703, 1993.
- [27] P. Bruno, “ELCCSTF accreditation proposal: PJM Package C,” PJM Interconnection, 2025. [Online]. Available: <https://tinyurl.com/pjmelcc>
- [28] ISO New England, “FCA 18 Demand Curves Data,” 2023. [Online]. Available: https://www.iso-ne.com/static-assets/documents/2023/08/a03_2023_08_23_pspc_fca_18_demand_curves.xlsx
- [29] New York Independent System Operator, “ICAPWG capacity accreditation presentation,” https://www.nyiso.com/documents/20142/33857891/02a_10-19-22%20ICAPWG%20Capacity%20Accreditation.pdf, 2022.
- [30] RTS-GMLC, “The Reliability Test System of the Grid Modernization Laboratory Consortium,” <https://github.com/GridMod/RTS-GMLC>.
- [31] N. Schlag, Z. Ming, A. Olson *et al.*, “Capacity and reliability planning in the era of decarbonization: Practical application of effective load carrying capability in resource adequacy,” *Energy and Environmental Economics, Inc.*, <https://www.ethree.com/elcc-resource-adequacy>, 2020.